Acta Neuropathol (2010) 119:617–630
DOI 10.1007/s00401-010-0644-7

ORIGINAL PAPER

Canine distemper virus persistence in demyelinating encephalitis by swift intracellular cell-to-cell spread in astrocytes is controlled by the viral attachment protein

Gaby Wyss-Fluehmann · Andreas Zurbriggen · Marc Vandevelde · Philippe Plattet

Received: 17 December 2009 / Revised: 14 January 2010 / Accepted: 19 January 2010 / Published online: 2 February 2010

Abstract The mechanism of viral persistence, the driving force behind the chronic progression of inflammatory demyelination in canine distemper virus (CDV) infection, is associated with non-cytolytic viral cell-to-cell spread. Here, we studied the molecular mechanisms of viral spread of a recombinant fluorescent protein-expressing virulent CDV in primary canine astrocyte cultures. Time-lapse video microscopy documented that CDV spread was very efficient using cell processes contacting remote target cells. Strikingly, CDV transmission to remote cells could occur in less than 6 h, suggesting that a complete viral cycle with production of extracellular free particles was not essential in enabling CDV to spread in glial cells. Titration experiments and electron microscopy confirmed a very low CDV particle production despite higher titers of membrane-associated viruses. Interestingly, confocal laser microscopy and lentivirus transduction indicated expression and functionality of the viral fusion machinery, consisting of the viral fusion (F) and attachment (H) glycoproteins, at the cell surface. Importantly, using a single-cycle infectious recombinant H-knockout, H-complemented virus, we demonstrated that H, and thus potentially the viral fusion complex, was necessary to enable CDV spread. Furthermore, since we could not detect CD150/SLAM expression in brain cells, the presence of a yet non-identified glial receptor for CDV was suggested. Altogether, our findings indicate that persistence in CDV infection results from intracellular cell-to-cell transmission requiring the CDV-H protein. Viral transfer, happening selectively at the tip of astrocytic processes, may help the virus to cover long distances in the astroglial network, "outrunning" the host's immune response in demyelinating plaques, thus continuously eliciting new lesions.

Keywords Demyelinating encephalitis · CDV persistence · Primary brain cells · Swift cell-to-cell spread · Attachment protein

G. Wyss-Fluehmann · M. Vandevelde
Division of Neurology, Vetsuisse Faculty, University of Bern, Bern, Switzerland

A. Zurbriggen · P. Plattet (✉)
Department of Clinical Research and Veterinary Public Health, Vetsuisse Faculty, University of Bern, Bremgartenstrasse 109a, 3001 Bern, Switzerland
e-mail: philippe.plattet@itn.unibe.ch

Introduction

Canine distemper virus (CDV) is an enveloped, non-segmented, negative-stranded RNA morbillivirus, closely related to measles virus (MV) and belongs to the family of the *Paramyxoviridae* [18]. Brain infection with CDV induces a chronic demyelinating disease which is considered to be a model for multiple sclerosis (MS) [36]. An infectious cause of MS, the most important inflammatory demyelinating disease in human, is suggested by epidemiological data but remains elusive [15]. White matter destruction in MS results from the inflammatory response, which is thought to be associated with autoimmunity against myelin antigens [19], but there is also evidence for intrathecal production of anti-viral antibodies [2]. In animal models of viral-induced demyelination, such as distemper, inflammatory white matter lesions result at least in part from the intrathecal immune response against the virus, which in the case of CDV infects predominantly astrocytes [39, 43]. However, previous studies performed with CDV have demonstrated that despite effective clearance of the virus in inflammatory lesions in the white matter of infected dogs [1], the virus has the ability to

spread to other areas of the central nervous system (CNS), ever eliciting new lesions [39]. Thus, viral persistence is the driving force behind the progression of the disease [29]. Unraveling the molecular mechanisms of viral persistence is therefore the key to understand the pathogenesis of chronic progressive inflammatory demyelination.

How CDV can establish a persistent infection in the CNS is poorly understood. Production of defective viruses such as in persistent CNS infection by the closely related MV in humans [29] does not occur in distemper [24]. Tissue culture studies suggested that virulent CDV shares the ability with MV to spread from cell-to-cell [43], a mechanism which may shield the infection from immune detection [34]. While cell-to-cell spread in models of MV infection occurs in neurons [21], CDV primarily infects astrocytes of the white matter [39, 44]. Our previous work suggested that viral persistence mediated by A75/17-CDV (a highly neurovirulent and demyelinating strain) in dog brain cell cultures (DBCCs) was characterized by a non-cytolytic infection with limited production of extracellular viral particles. Infected cells were widely spaced but seemed to be in contact with each other by their processes thus indicating cell-to-cell spread [43, 44]. These findings were suggestive of a different mechanism of viral transmission of persistent CDV as compared to cytolytic CDV strains.

In the present study, we infected primary canine brain cell cultures with a recombinant red fluorescent protein (RFP)-expressing wild-type Morbillivirus strain (rA75/17^{red}) to investigate the mechanism of persistent CDV infection. Fluorescent protein-expressing CDV strains have been used before in vitro [25] as well as in vivo [32, 40]. Our results indicated that spread of persistent CDV in astrocytes did not require infectious particles, whereas the viral attachment protein was crucial in allowing lateral cell-to-cell transmission most likely by mediating cell–cell fusion activity. Furthermore, we found that viral spread to neighboring cells could occur in very short time, supporting the notion that lateral cell-to-cell transmission of CDV in brain cells is highly efficient.

Materials and methods

Cells and viruses

Primary DBCCs were prepared as previously described [44]. Vero-SLAM cells (kindly provided by V. von Messling, INRS-Institut Armand-Frappier, University of Quebec, Laval, Quebec, Canada) were grown in multiwell plates, for some experiments with coverslips attached to the bottom of the wells. Tissue culture medium consisted of Dulbecco's modified Eagle medium (DMEM, Invitrogen) supplemented with 10% fetal calf serum (FCS), penicillin and streptomycin. The selection of Vero cells expressing the SLAM receptor was maintained by adding Zeocin^{TM} (Invitrogen). Cells were kept at 37°C in the presence of 5% CO_2. The recombinant (rA75/17^{red}) virus contains an additional red fluorescence marker gene (RFP: "tD-tomato", a kind gift from D. Garcin, University of Geneva [22]) located between the M and F genes (rA75/17^{red}) and was amplified in Vero-SLAM cells. The recombinant A75/17 virus, containing an additional RFP gene and additionally knocked out for the hemagglutinin gene, was amplified via *trans*-complementation with the wild-type hemagglutinin protein (Hwt), in Vero-SLAM cells stably expressing Hwt (rA75/17^{red} H^{ko}/H^{comp}, allowing the generation of single-cycle infectious viruses).

Cultures of primary dog brain cells were infected as soon as they reached confluency (which was between days 5 and 7 post-seeding) at an MOI of 0.01 (titrated in Vero-SLAM cells) with rA75/17^{red} for 2 h. In several experiments, infected cultures were overlaid 1 day post-infection (dpi) with medium containing soft agar (1%) to inhibit free movement of extracellular viral particles.

Generation of CDV full-length cDNA clones

The plasmid containing the full-length cDNA clone of the A75/17-CDV genome (pA75/17 [30]) was digested with *Bst*EII. A small linker containing the unique restriction site *Apa*I was generated by annealing two single-stranded DNA oligonucleotides and subsequently cloned into the *Bst*EII-cleaved pA75/17 plasmid. The RFP gene (tD-tomato, kindly gift by D. Garcin, University of Geneva, Switzerland) was next amplified by conventional PCR technique and cloned into the *Apa*I-cleaved vector, thus generating pA75/17^{red}. Next, plasmid pA75/17^{red} was digested with *Mlu*I and *Bss*HII. Again, a small linker was generated by annealing two single-stranded DNA oligonucleotides and subsequently cloned into the cleaved pA75/17^{red} plasmid, thus generating pA75/17^{red}-H^{ko}. Both full-length cDNA clones respect the rule of six [5]. Primer sequences are available upon request. Viruses were rescued as previously described [28] with minor modification in case of rA75/17^{red}/H^{ko}/H^{comp}, as detailed in "Results".

Generation of Hwt-expressing Vero-SLAM cells (Vero-SLAM-H)

Vero-SLAM cells were transduced with pRRL lenti vectors at an MOI of 5. Consequently, a Vero-SLAM-Hwt clone was selected by limiting dilution and was used for further experiments. Flow cytometry analysis using two conformational epitope-recognizing anti-CDV-H MAbs (3900 [26] and 1C42H11, VMRD) were employed to confirm Hwt expression at the cell surface.

The lentivirus vector pRRL has been described elsewhere [6], and kindly provided by Patrick Salomon, University of Geneva). Stocks of lentivirus vectors were generated in 293T/17 cells as previously described [6].

Confocal fluorescence microscopy and video microscopy

Dog brain cell cultures infected with the rA75/17^{red} were examined by confocal fluorescence microscopy (Olympus) at 3, 6, 9 and 12 dpi. At 3 dpi, several infected foci were selected and their locations (x–y axis) were stored using a coordination software package (Fluoview FV1000, Version 1.7b). At each consecutive time point, the identical foci were thus tracked, photographed and the viral spreading pattern analyzed.

For the life cell video imaging procedure, DBCCs were placed in a life imaging system incubator chamber. Foci of infection with rA75/17^{red} in DBCCs were determined at 3 dpi. Images were taken at 1 h intervals from the same infected foci during 72 h (Nikon TE2000E-PFS, Hamamatsu ORCA-AR Camera, and Nikon NIS Elements Software).

Immunofluorescence

At 3, 6, 9 and 12 dpi, DBCCs on coverslips were washed with PBS and subsequently fixed with PBS containing 4% paraformaldehyde. Cells were washed, permeabilized with normal goat sera 5% containing Triton-X 100 (0.5%) for 20 min and further blocked for 1 h with 5% goat sera in PBS. Then, either one of the following primary antibodies was added to the cells: mouse monoclonal anti-N (D110 [1]), rabbit polyclonal anti-glial fibrillary acidic protein (DAKO®, Zug, Switzerland), rabbit polyclonal anti-canine SLAM protein [42], mouse monoclonal anti-H glycoprotein (3900 [26]) or mouse monoclonal anti-F (4068 [26]) glycoprotein. Furthermore, in some experiments, the same procedure was used to stain Vero and Vero-SLAM cell cultures for assessing SLAM expression. As secondary antibodies, either anti-mouse IgG (Alexa Fluor® 488, Invitrogen®) or anti-rabbit IgG fluorescent antibodies (Alexa Fluor® 555, Invitrogen®) were employed. In addition, Toto®-3 iodide (Invitrogen®) was added for nuclear staining.

Electron microscopy

Material from a previous experiment designed to study oligodendroglial pathology in CDV infection was re-examined. Briefly, A75/17-CDV-infected DBCCs grown in petri dishes had been harvested at various intervals post-infection, fixed with glutaraldehyde, detached from the petri dish and pelleted by centrifugation. The pellets had been osmicated and embedded in resin. Thin sections were examined with an electron microscope. Representative areas had been photographed at various magnifications. These images were re-evaluated in the present study specifically focusing on morphological aspects of CDV replication especially searching for signs of budding, viral particles, localization of nucleocapsids and cell–cell membrane fusion.

RT-PCR

Total RNA extraction was performed from infected and non-infected DBCCs, Vero or Vero-SLAM cells, using the RNA extraction kit (Qiagen). Subsequently, reverse transcription (Roche) and the PCR amplification (Roche) were made according to the manufacturer's instructions. The primers used for SLAM and GAPDH amplification are available upon request. Finally, PCR products were submitted to migration on a 1% gel agarose.

Growth kinetics and virus titration

To assess the growth kinetics of the viruses in DBCCs, samples were taken at 3, 6, 9, 12 and 15 dpi. Titers of both the cell-free (SN) and cell-associated (CA) viruses were examined. Cell-free viruses were directly harvested from the supernatant of infected cells, centrifuged at 2,000 rpm and stored at −80°C. Cell-associated viruses were released by two cycle of freezing/thawing, centrifuged at 2,000 rpm and subsequently stored at −80°C. Titration experiments were performed on Vero-SLAM cells by limiting dilution assay, as previously described [27].

Generation of lentiviral vector expressing the CDV receptor CD150/SLAM and Hwt

The lentivirus vector pRRL has been described elsewhere ([6], and was kindly provided by Patrick Salomon, University of Geneva). The SLAM gene was amplified by PCR (Roche) and subsequently digested with *Rsr*II and cloned into the pRRL-RsrII-cleaved vector. Stock of lentivirus vectors was generated in 293T/17 cells as previously described [6]. The identical strategy was used to clone the Hwt gene into the pRRL vector. Hwt was amplified by conventional PCR technique (Roche) from the expression vector pCI-Hwt [27].

Results

In primary DBCCs, the demyelinating A75/17-CDV strain spreads from cell-to-cell in a selective manner by way of cell processes

Primary DBCCs, mainly consisting of astrocytes, were confluent 1 week after seeding. At that time point, they

were infected with the recombinant A75/17-CDV engineered to express the RFP (rA75/17^{red}) from an additional transcription unit located between the M and F genes. Foci of infection were identified 3 dpi and localized by confocal laser scanning microscopy combined with a coordinate software package allowing tracking identical foci at consecutive time intervals. Selected foci were photographed every 3 days. Figure 1a–d illustrates a typical example of the evolution of one infected focus over time. Infected cells and their finely branching processes were outlined by the RFP and did not exhibit any signs of syncytia formation and cytolysis. Infected foci became steadily larger but generally with wide spacing between infected and target cells, leaving immediately surrounding neighboring cells uninfected. Importantly, infected cells seemed always to be in contact with each other by way of their processes. Confocal laser microscopic images representing thin horizontal slices of the culture often revealed continuity between infected cells and processes (Fig. 1e, f). Immunofluorescence analysis in rA75/17^{red}-infected DBCCs, using an antibody against the N protein of CDV, revealed perfect congruency of the RFP with presence of the viral protein, thus excluding passive diffusion of the RFP to non-infected cells (Fig. 1g). In addition, immunofluorescence analysis indicated that the main target of rA75/17^{red} in DBCCs was astrocytes (Fig. 1h), consistent with our previous reports [39]. Furthermore, astrocytic processes could exhibit positive particulate immunofluorescent signals when stained with an anti-N (nucleoprotein) monoclonal antibody (MAb) (Fig. 1i, j), presumably representing viral nucleocapsid aggregates.

To more accurately track non-cytolytic viral spread and to visualize dynamic changes within short intervals, we performed time-lapse video microscopy. To this aim, 3 days after initial infection, images were taken from infected foci every hour during a period of 3 days. The speed of intercellular viral transmission was highly variable and appeared to take place in leaps and bounds. Infected foci could remain quite stable for many hours or even days and then suddenly start to spread to other cells in a few hours. This is illustrated in Fig. 2, which shows an example of rA75/17^{red} cell-to-cell spread tracked with 1 h intervals. The focus of infection started from two initially infected cells, which were expressing RFP already at 72 hpi but with the infection remaining quite inactive until 90 hpi. Using this approach, it became clear that transmission of the infection strictly implicated two contacting cells and that the infection was transmitted by the tip of a cell process from an infected cell contacting a target cell. In the latter, fluorescence became first visible in the cell body and later in the cell processes, which then transmitted the infection to a third remote cell. Remarkably, time-lapse video microscopy revealed in some foci that CDV could spread to remote cells within a matter of 5–6 h (Fig. 2, initial infected cell, red arrowhead; remotely infected cells, yellow and blue arrowheads). This is much shorter as compared to 24 h that are in general required for CDV to produce free viral particles that can subsequently re-infect a new cell [12].

The above results taken together suggest that, in primary canine brain cells, the RFP-expressing recombinant CDV spread laterally from cell-to-cell in a non-cytolytic and selective manner by way of cell processes.

The canine CD150/SLAM receptor is not expressed in DBCCs

To date, the CD150/SLAM receptor is the only known receptor for virulent CDV [37, 38, 41]. Previous studies suggested paucity of SLAM expression in brains of uninfected dogs but that SLAM expression might be upregulated in brain of dogs with distemper [42]. Since we demonstrated that rA75/17^{red} spread very efficiently in DBCCs, we investigated whether SLAM was expressed and/or upregulated in primary dog brain cells upon infection. Since SLAM detection by immunofluorescence analysis remained repeatedly negative (data not shown), we employed a more sensitive technique to monitor SLAM expression. Thus, RT-PCRs from extracted DBCCs RNA were performed from infected and non-infected cells at six consecutive time points post-infection (0, 3, 6 and 9, 12 and 15 dpi). To validate our SLAM primers, RNAs extracted from Vero and Vero-SLAM cells served as negative and positive control, respectively, and semi-quantitative RT-PCRs were performed by including the analysis of the housekeeping GAPDH gene. Figure 3 clearly documents that SLAM mRNA was totally undetectable throughout the whole course of a successful infection with rA75/17^{red} in DBCCs, whereas the GAPDH mRNA in the identical samples was constantly detected, thereby validating our semi-quantitative RT-PCR system. Combined, these results not only demonstrate that the SLAM receptor was absent from primary canine brain cells but that efficient infection did not upregulate its expression.

Extremely limited free viral particle formation and inefficient cell entry of rA75/17^{red} in DBCCs

We then determined the kinetics of infectivity of rA75/17^{red} in DBCCs during a period of 2 weeks. In these series of experiments, both cell-free (SN) and cell-associated (CA) viruses were analyzed. Figure 4a illustrates the kinetics of virus titers, which were determined in Vero-SLAM cells. The titer of supernatant viral particles reached a maximum of 10–30 infectious units per ml at day 9

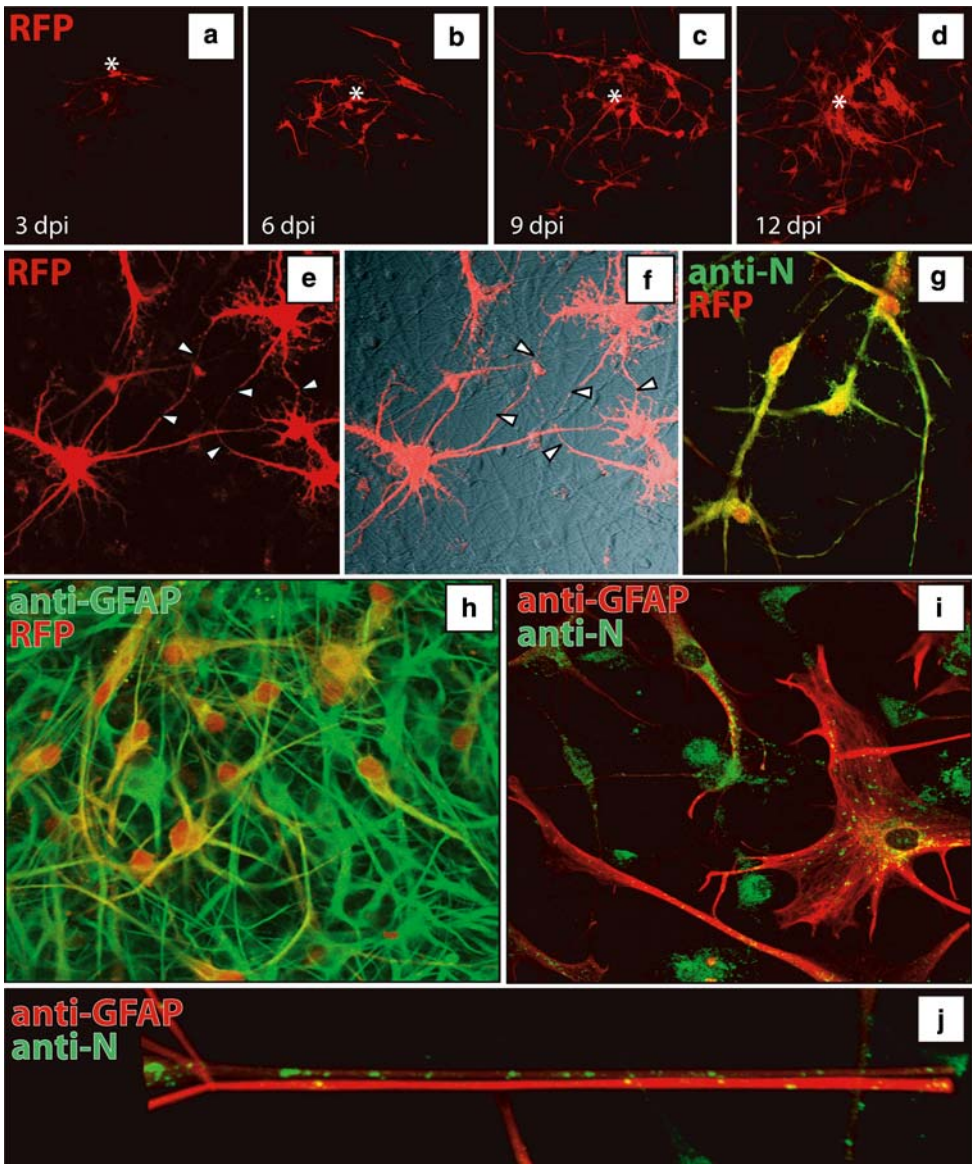

Fig. 1 Spread of rA75/17^{red} in primary dog brain cell cultures (DBCCs). **a–d** The recombinant A75/17-CDV, expressing an additional red fluorescent protein (rA75/17^{red}), efficiently spreads in DBCCs. A growing infected focus is shown at 3, 6, 9 and 12 dpi. *Asterisk* depicts the same coordination point throughout the time of infection. Red fluorescence emission outlines the whole infected cells and their processes. Infected cells are widely spaced but seem always in contact with each other by way of their processes. Confocal laser microscopy ×20. **e** rA75/17^{red}-infected DBCCs are in contact through thin cell processes (*white arrowheads*), as observed by the red fluorescence emission. Confocal laser microscopy ×200. **f** Merged images of CDV-induced red fluorescence emission and corresponding DIC image demonstrating that the DBCCs are confluent with spread of CDV from infected to target cells bypassing numerous uninfected cells. Confocal laser microscopy ×200. **g** Merged images of CDV nucleoproteins (N) labeled with a primary anti-N antibody, followed by a secondary alexa fluor 488-conjugated antibody (*green*), with red fluorescence emission in rA75/17^{red}-infected cells (*red*) shows co-localization of both labels (*yellow*) excluding passive diffusion of RFP. Confocal laser microscopy ×200. **h** Astrocytes are the main target of rA75/17^{red} in DBCCs. Merged images of CDV-infected cells by direct emission of red fluorescence (*red*) and astrocytes stained with an anti-GFAP antibody, followed by a secondary alexa fluor 555-conjugated antibody. **i** The CDV nucleocapsids (*green*) are located both in the cytosol and processes of infected astrocytes (*red*). Merged images of CDV nucleoprotein (N) stained with an anti-N antibody, followed by a secondary alexa fluor 488-conjugated antibody and astrocytes stained with an anti-GFAP antibody, followed by a secondary alexa fluor 555-conjugated antibody. Confocal laser microscopy ×200. **j** 3D reconstruction of 30 Z stacking images taken by confocal laser microscopy illustrating the presence of CDV nucleocapsids [anti-N antibody staining, followed by alexa fluor 488-conjugated antibody (*green*)] inside thin long astrocytic processes [anti-GFAP antibody staining, followed by alexa fluor 555-conjugated antibody (*red*)]. Confocal laser microscopy ×1,000

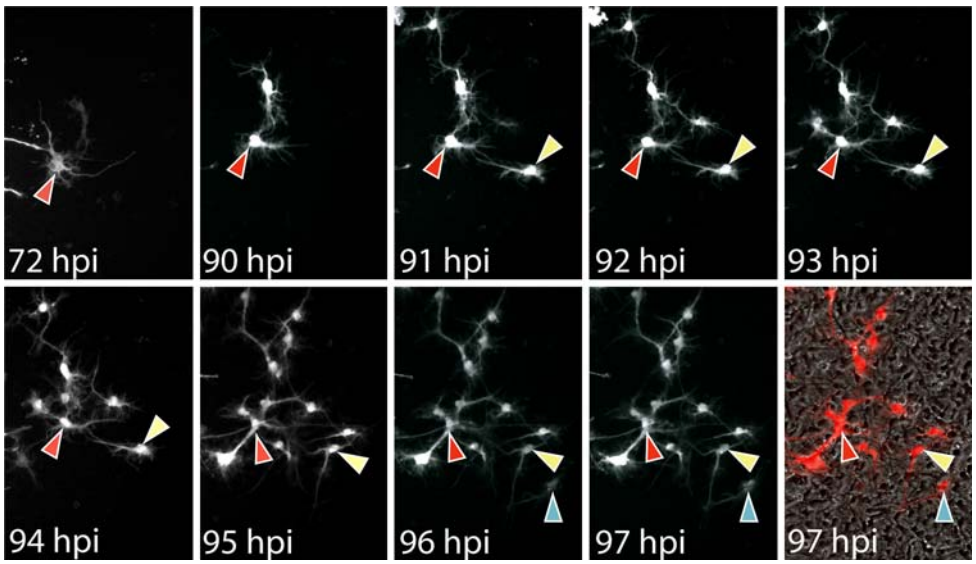

Fig. 2 Video microscopy of DBCCs infected with rA75/17^{red}. Consecutive images of an infected focus taken at 1 h intervals (or 18 h; *two first images*). *Red arrowhead* depicts an infected cell at the beginning of the sequence (72 h post-infection). From 90 hpi, the infection is spreading to other cells by contact of cell processes in various directions. Additional cells become fluorescent within intervals of 1 h. The *yellow arrowhead* depicts one of these cells (91 hpi). A process of the latter becomes fluorescent at 95 hpi. One hour later (96 hpi), the latter is in contact with a process of an additional cell (depicted by *blue arrowhead*), now becoming fluorescent. The last image of the series (104 hpi) illustrates an overlay of the red fluorescent protein with phase contrast showing a confluent culture, thereby demonstrating that the infection spreads selectively bypassing numerous cells which remain uninfected (×40)

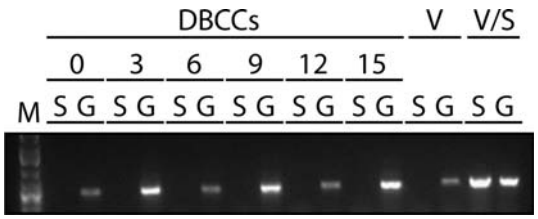

Fig. 3 The universal *Morbillivirus* CD150/SLAM receptor is not expressed in primary canine brain cells. DBCCs were infected (or left uninfected) with rA75/17^{red} at an MOI of 0.01 (as titrated in Vero-SLAM cells). Total RNA was then extracted and subjected to RT-PCRs for assessing SLAM and the housekeeping gene GAPDH expressions at the indicated days post-infection. In addition, total RNA was extracted from Vero and Vero-SLAM cells to control for any defect in the RT-PCR system. *S* SLAM gene, *G* GAPDH gene, *V* Vero cells, *V/S* Vero-SLAM cells

post-infection. This can be regarded as an insignificant amount with respect to the much higher cell-associated infectious titers (3×10^4). Next, we sought to determine the entry efficiency of rA75/17^{red} in cultured astrocytes by infecting Vero-SLAM cells and DBCCs with an equal amount of viruses (MOI of 0.01 as titrated in Vero-SLAM cells). One day post-infection, the number of infected cells per well were then counted. While infection of Vero-SLAM cells with rA75/17^{red} produced about 20,000 infected cells, only 200 were counted in DBCCs (Fig. 4b). Thus, viral particles of the virulent virus entered glial cells in a very inefficient manner as compared to cells expressing the canine CD150/SLAM receptor.

The results of titration and viral cell entry analyses strongly argue against viral cell-to-cell transmission being sustained by way of extracellular viral release. Moreover, this conclusion was further supported by covering infected DBCC with medium containing agar, limiting free movement of released infectious particles. Despite mild cytotoxicity of the agar overlay on brain cells, cell-to-cell spread of rA75/17^{red} in DBCCs remained efficient (not shown). Finally, we searched for viral budding in astrocytes by electron microscopy, which is easily demonstrated after infection with the highly cytolytic Onderstepoort CDV strain [11]. Strikingly, however, viral budding was extremely rare in case of rA75/17^{red}-infected DBCCs, confirming our titration assays in supernatants. Nevertheless, massive numbers of nucleocapsids were detected in the cytosol of perikarya, cell processes and their finest ramifications (Fig. 5a–f, white arrowheads). These nucleocapsids were easily found as small and large aggregates of typical tubular structures of the "fuzzy" type (Fig. 5a, b, e) as described in the literature [3]. In such aggregates, nucleocapsids were either surrounded by clear cytosol and cell organelles (Fig. 5b, white arrowhead) or embedded in a granular electron-dense matrix (Fig. 5c, d, white arrowheads). The latter type of inclusions was very often attached to the plasma membrane (Fig. 5d, white arrowhead). Occasionally, alignment of nucleocapsids along the cell membrane could be observed as well as focal, sometimes discontinuous, plasmalemmal densities, reminiscent

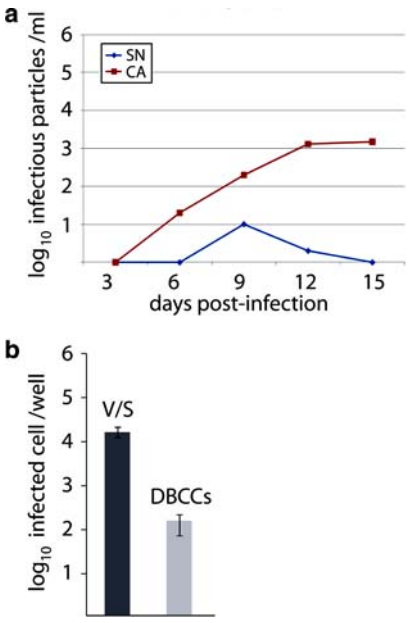

Fig. 4 rA75/17^{red} is defective in free particles formation in primary canine brain cells. **a** DBCCs were infected with rA75/17^{red} at an MOI of 0.01 (as titrated in Vero-SLAM cells). At the indicated days post-infection, cell-free (SN) and cell-associated viruses (CA) were harvested and titrated. Virus titers were determined 3 dpi by counting the number of virus-infected cells (RFP-expressing cells). The cells were overlaid 2 h post-infection with medium containing 1% of soft agar. Values represent the mean of three independent experiments. **b** Virus entry efficiency. Vero-SLAM cells (V/S) and DBCCs were infected with rA75/17^{red} at an MOI of 0.01 (titrated in Vero-SLAM cells). One day post-infection, the number of infected Vero-SLAM cells and DBCCs per well were counted and are represented in the graph

of insertion of viral surface proteins, described as "spiking" (Fig. 5e, grey arrowheads), in cytolytic infection [12]. Thus, all these findings confirmed full replication of rA75/17^{red} in DBCCs but with extremely rare formation of viral particles. Cell–cell fusion with formation of multinucleated cells was not observed in the time frame of the experiments described above. Focal blurring of the cell borders in two opposing cytoplasmic membranes of infected cells was sometimes seen (Fig. 5b, grey arrowhead, c, small white arrowheads). Cell processes connecting infected cells establishing continuity between them, as suggested by the confocal laser microscopy images, were difficult to demonstrate since the chance of finding two widely separated cells with connecting cell processes in the same plane of section at the ultrastructural level is extremely small. Figure 5f is a composite image of four overlapping EM photographs showing such a cell process (white arrows).

Taken together, these data support strong evidence that rA75/17^{red} non-cytolytic cell-to-cell spread in primary canine brain cells is not mediated by viral free particle formation but rather through direct contact with neighboring cells associated with transfer of viral nucleocapsids.

Both viral surface glycoproteins are expressed, surface-targeted and functional in DBCCs

It is plausible that the viral fusion machinery, which consists of the fusion (F) and attachment (H) proteins, could be involved in the direct intercellular transfer of CDV by establishing pores between an infected and a target cell. However, syncytia, an easily visible proof of cell–cell fusion in cytolytic CDV infection [44], are absent in the persistent infection. Therefore, following immunofluorescence demonstration of H and F expression in infected glial cells (Fig. 6a, b), we further investigated whether both glycoproteins were properly surface-expressed and functional. To this aim, we engineered a lentivirus vector expressing the canine CD150/SLAM receptor. The rationale behind this strategy was to assess whether rA75/17^{red} could mediate syncytia formation in SLAM-transduced primary canine brain cells, which would reveal not only the production of functional F/H complexes but also their expression at the plasma membrane. As a transduction control, DBCCs were initially transduced with a GFP-expressing lentivirus. We noticed that the efficiency of lentivirus transduction in DBCCs was rather low, yielding a maximum of 5–10% of GFP-expressing cells (not shown). Nevertheless, DBCCs were first infected with SLAM-expressing (or empty) lentivirus vectors and cells were super-infected with rA75/17^{red} 3 days post-transduction. Strikingly, while in DBCCs transduced with the control empty vector, no syncytia were detected throughout the whole cell monolayer (Fig. 6c), small but clear syncytia could be readily observed in SLAM-transduced, rA75/17^{red}-infected, DBCCs (Fig. 6d).

Combined, these results indicated that functional viral fusogenic complexes were expressed at the plasma membrane in non-cytolytic infection mediated by rA75/17^{red} in primary brain cells.

The receptor-binding protein H is required for viral spread

The expression of functional fusion complexes on the cell membrane by itself is not sufficient to induce cell–cell fusion. The current model of paramyxovirus fusion and pore formation mechanism suggests that upon host cell receptor binding the attachment (H) protein triggers a signal to the fusion (F) protein, which in turn dramatically refolds to ultimately mediate membrane fusion activity [16, 17, 33]. Consistent with the notion that the receptor-binding H protein is central in the fusion model, we generated a recombinant virus with the attachment protein gene knocked out from the viral genome (rA75/17^{red} H^{ko}). This strategy, however, requires the production of single-cycle infectious virus to enable initial cell entry. We thus thought

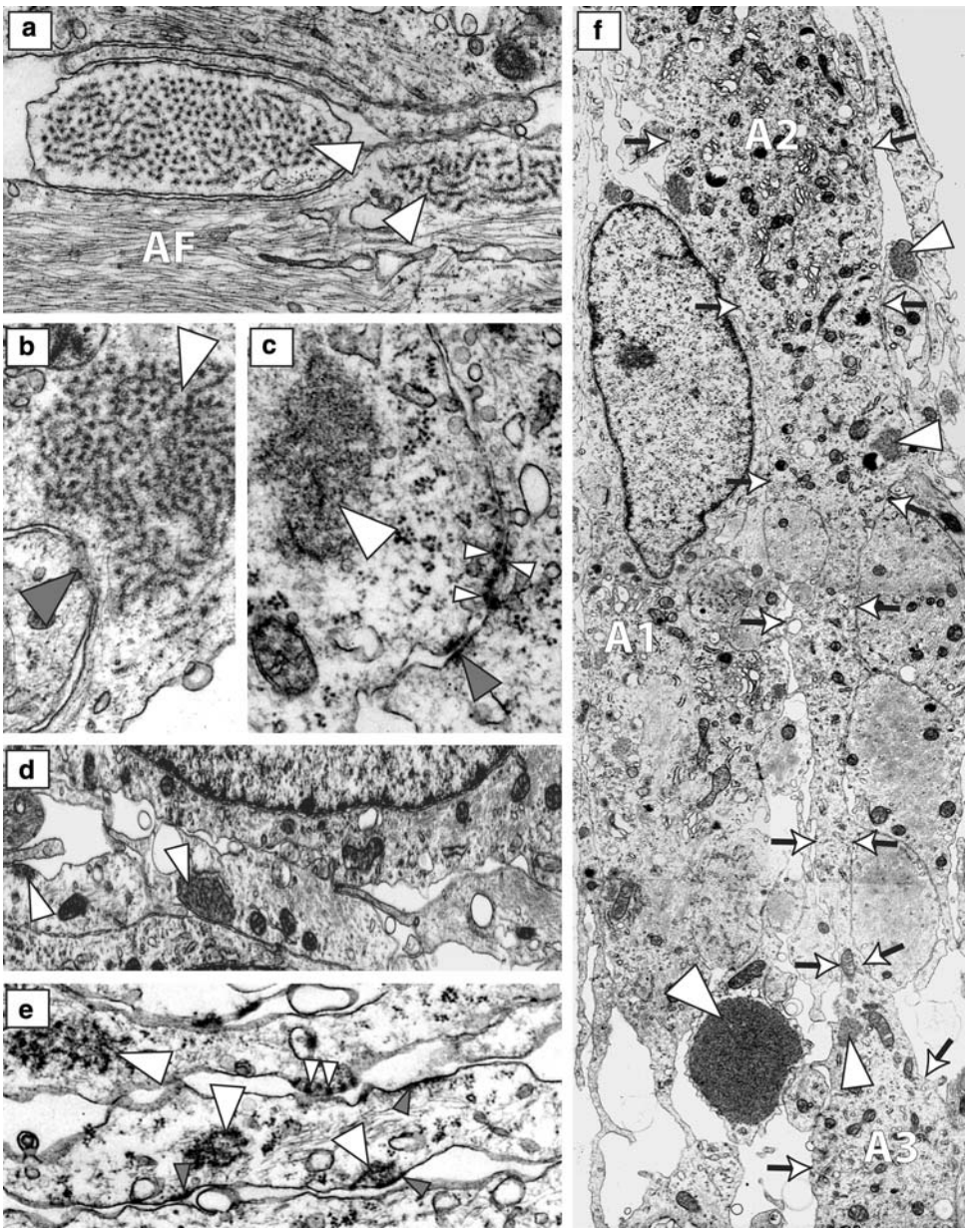

Fig. 5 Ultrastructural images of DBCCs infected with A75/17-CDV. **a** Large and small cell adjacent processes containing cross and longitudinally sectioned tubular profiles of CDV nucleocapsids (*arrowheads*). *AF* bundles of astrocytic fibrils (×11,000). **b** Two adjacent astroglial cell processes. In the cytosol of the left process accumulation of "fuzzy" nucleocapsids (*open arrowhead*) close to cell membrane with focal blurring of the adjacent cell membranes between the two cells (×15,000). **c** Two adjacent cell processes. The upper process contains an electron-dense nucleocapsid aggregate. Discontinuous plasmalemmal densities, "spiking" (*filled arrowheads*), distinction between adjacent cell membranes becomes less clear in this area. *Arrow* depicts nearby gap junction (×11,000). **d** Cell process between two cell bodies containing electron-dense nucleocapsid aggregates with tubular structures embedded in a granular matrix (*arrowheads*) attached to the cell membrane (×11,000). **e** Several closely spaced cell processes, containing nucleocapsid aggregates (*open arrowheads*). Several plasmalemmal densities (*grey arrowheads*), one of which exhibits "spiking" morphology (*double arrowhead*) (×11,000). **f** Low power composite of four overlapping EM photographs showing an astrocyte with nucleus (A1) and parts of the perikaryon of two further astrocytes (A2, A3) all of which contain numerous nucleocapsid aggregates (a few depicted by *white arrowheads*) (×3,000). In addition, the image shows several large and small cell processes equally containing nucleocapsid aggregates and one large viral inclusion (*double white arrowhead*). *Small arrows* depict a cell process connecting A2 and A3 with continuity between the cytoplasm of both perikarya

to complement the particles by introducing H in *trans* using Vero-SLAM cells that constitutively express the receptor-binding H protein. The latter cells were obtained by transducing Vero-SLAM cells with a lentivirus expressing Hwt. Though the different resulting clones exhibited only low level of H expression at the cell surface, most of the

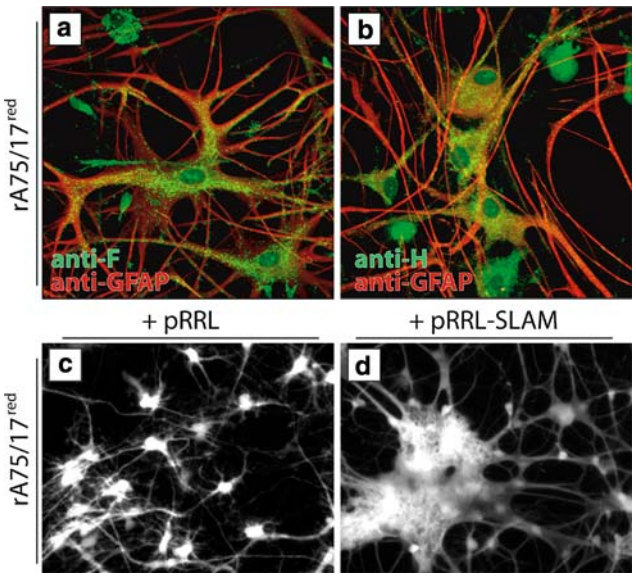

Fig. 6 The CDV fusogenic complexes are potentially functional in DBCCs. **a**, **b** Both CDV surface glycoproteins are properly expressed in glial cells. DBCCs were infected with rA75/17^{red} with an MOI of 0.01. Merged images of both glycoproteins F and H stained with anti-F and anti-H antibodies, respectively, followed by secondary alexa fluor 488-conjugated antibody (*green*) and astrocytes labeled using an anti-GFAP antibody, followed by a secondary alexa fluor 555-conjugated antibody (*red*). Confocal laser microscopy ×200. **c**, **d** F/H complexes are cell surface targeted in potentially functional. Prior to infection of DBCCs with rA75/17^{red} (MOI of 0.01), cells were transduced with a lentivirus vector expressing SLAM (pRRL-SLAM) or with a control empty plasmid (pRRL). Syncytia formation was readily observed in CDV-infected cells. No syncytia are demonstrated in the control culture

clones elicited positive staining as determined by immunofluorescence analysis (data not shown). This was followed by limited dilution, which allowed us to select a clone named Vero-SLAM-H. Flow cytometry analysis using two different conformation-dependent anti-H MAbs validated Hwt expression at the cell surface. Furthermore, we also confirmed that SLAM was not dramatically down-regulated (not shown). Hwt and SLAM functionalities were finally assessed by transfecting Fwt in Vero-SLAM-H cells. Indeed, cell–cell fusion activity was readily induced (not shown).

Bsr-T7 cells [4] were used for transfection with the different plasmids necessary and sufficient to initiate the viral life cycle (pTM-N, P, L and the relevant full-length cDNA [28]). Importantly, the expression plasmid encoding the VSV glycoprotein G was added to the transfection mixture. VSV-G was employed to pseudo-type CDV particles, in turn allowing the first transfer from Bsr-T7 to Vero-SLAM-H cells in a VSV-G-dependent manner. Three successive passages in Vero-SLAM-H cells were then performed to amplify the H-knockout virus in the absence of VSV-G. Using this strategy, we could successfully rescue a virus that we named rA75/17^{red} H^{ko}/H^{comp}, which reached titers of about 1 × 10^4 viruses/ml.

To verify whether the newly recovered recombinant virus was indeed *trans*-complemented by H but impaired in H protein expression, Vero-SLAM and Vero-SLAM-H cells were infected with wild-type rA75/17^{red} or with rA75/17^{red} H^{ko}/H^{comp}, respectively. Immunofluorescence analyses using the anti-H MAb (3900 [26]) were then performed on fixed and permeabilized cells, 30 h post-infection. Importantly, red fluorescence could be observed with both viruses in Vero-SLAM and Vero-SLAM-H cells, indicating that both viruses efficiently entered and replicated (Fig. 7b, e, h, k). Moreover, this result supports the notion that H was incorporated in the recombinant H-knockout virus' envelope. As expected, rA75/17^{red} efficiently produced the receptor-binding H protein in both cell lines. Note that in Vero-SLAM-H cells, all cells (infected and non-infected) exhibited the anticipated positive staining for H. Conversely, in rA75/17^{red} H^{ko}/H^{comp}-infected Vero-SLAM cells, no H protein was detected at all by immunofluorescence analysis, whereas in Vero-SLAM-H cells positive staining was observed (Fig. 7a, d, g, j). Furthermore, in Vero-SLAM-H cells, rA75/17^{red} H^{ko}/H^{comp} mediated efficient syncytia formation thus validating proper F expression, whereas in Vero-SLAM cells infection was clearly restricted to the initially infected cell. Finally, anti-H MAbs (3900 and 1347 [26]) neutralized both viruses in both cell lines, confirming that H was anchored in both virus' envelopes and that F alone was not sufficient to support viral cell entry in these cells (data not shown). These results taken together validate that our newly recovered H-knockout rA75/17-CDV was indeed impaired in receptor-binding protein expression, while being *trans*-complemented by a functional H protein.

DBCCs were thus infected either with rA75/17^{red} or with rA75/17^{red} H^{ko}/H^{comp} at an MOI of 0.001. We constantly obtained a mean of 10–50 infected cells throughout the primary DBCCs with both recombinant viruses 1–2 dpi. As expected, rA75/17^{red} spread efficiently, since viral foci originating from single initially infected cells grew to more than 100 infected cells after 5–7 days of infection (see Fig. 1a). Strikingly, however, rA75/17^{red} H^{ko}/H^{comp} was totally deficient in cell-to-cell transmission, since viral infection remained restricted to the initially infected cells (Fig. 8a–d). Importantly, the obvious absence of diffusion of the RFP to contacting neighboring glial cells from rA75/17^{red} H^{ko}/H^{comp}-infected cells provided strong evidence that potentially pre-existing astrocytic connections were insufficient to allow transfer of small molecules such as RFPs, thereby excluding any spontaneous transfer of large macromolecules such as viral nucleocapsids.

To confirm the above data, we sought to determine whether MAbs directed against the receptor-binding H

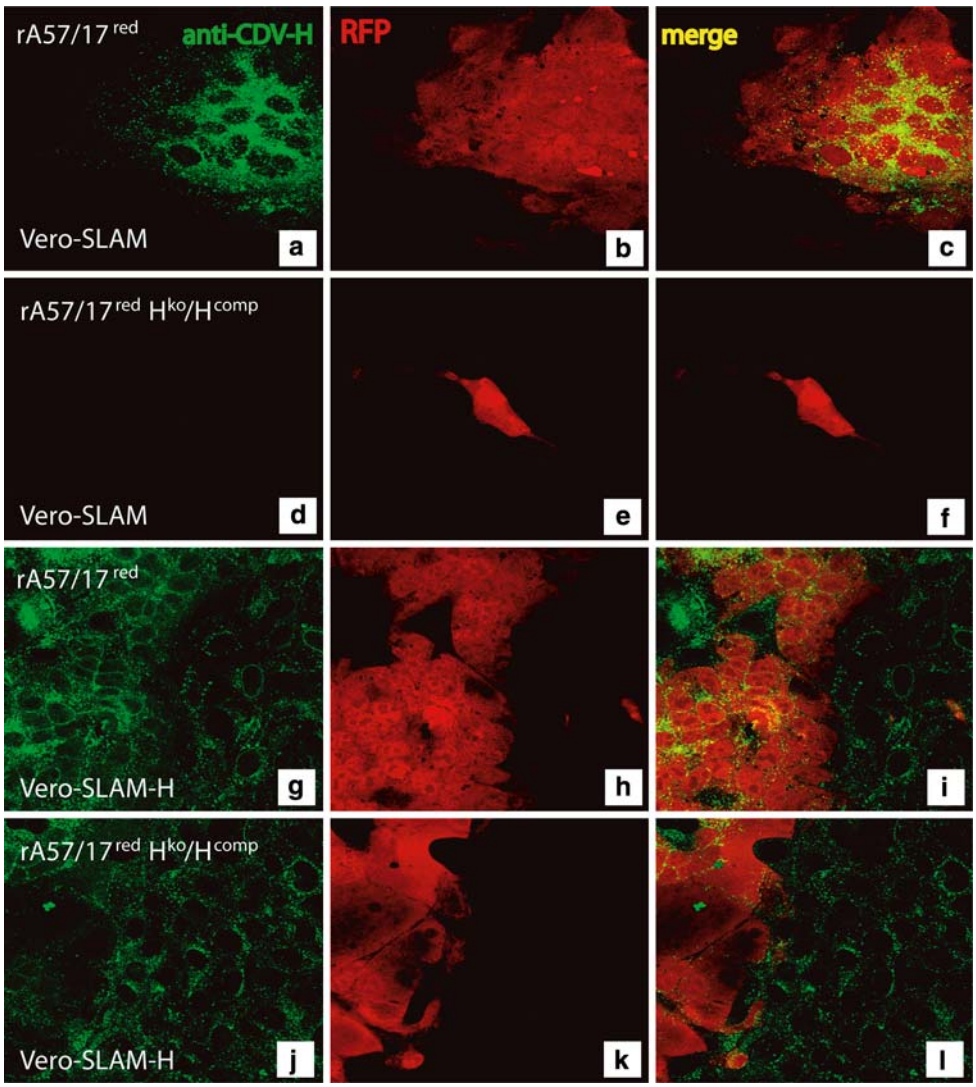

Fig. 7 Characterization of the recombinant H^{ko} rA75/17^{red} virus. Vero-SLAM (**a**–**f**) and Vero-SLAM-H cells (**g**–**i**) were infected with rA75/17^{red} and rA75/17^{red}/H^{ko}/H^{comp}. One day post-infection, both cells were fixed, permeabilized and stained using the anti-H MAb 1C42H11 (VMRD) to detect the CDV hemagglutinin protein. This was followed by addition of an alexa fluor 488-conjugated secondary antibody. In addition, auto-fluorescence of the RFP is also shown, which allowed us for a direct illumination of infected cells. Merged images are also represented (**c**, **f**, **i** and **l**). Fluorescent images were taken using a confocal scanning laser microscope (Olympus) (×200)

protein could also inhibit cell–cell transmission. Hence, several MAbs were initially tested in F/H-transfected Vero-SLAM cells to assess their potential to inhibit lateral cell–cell fusion activity. One out of four anti-H MAbs was able to strongly inhibit syncytia formation (MAb anti-H 1347 [26]). This antibody was thus tested in infected primary canine brain cultures. While a control antibody (anti-HA) did not influence rA75/17^{red} spread in DBCCs throughout the time of infection (Fig. 8e), the anti-H MAb 1347 strongly impaired viral cell–cell transmission (Fig. 8f), in turn confirming the key role of CDV-H in governing the non-cytolytic type of spread of virulent CDV in brain cells.

Taken together, this is the first demonstration for the morbilliviruses that the hemagglutinin (H) protein is strictly required for efficient viral spread in glial cells. These results further suggest that CDV-mediated fusion activity may be necessary to allow non-cytolytic cell-to-cell spread in brain cells, in turn excluding direct transfer of the nucleocapsid to neighboring cells through other pre-existing intercellular channels.

Discussion

To investigate the mechanism of viral cell-to-cell spread leading to persistence and chronic progressive demyelination [39], we used primary canine brain cell cultures combined with a molecularly cloned CDV, engineered to express an additional RFP, but otherwise identical in sequence to a virulent and demyelinating morbillivirus strain. Our results indicate that cell-to-cell spread does not require budding particles as in traditional viral life cycle models of CDV transmission [12]. Indeed, titration experiments demonstrated that persistent CDV in glial cells produces extremely low levels of free progeny viruses, which furthermore had very low entry efficiencies in

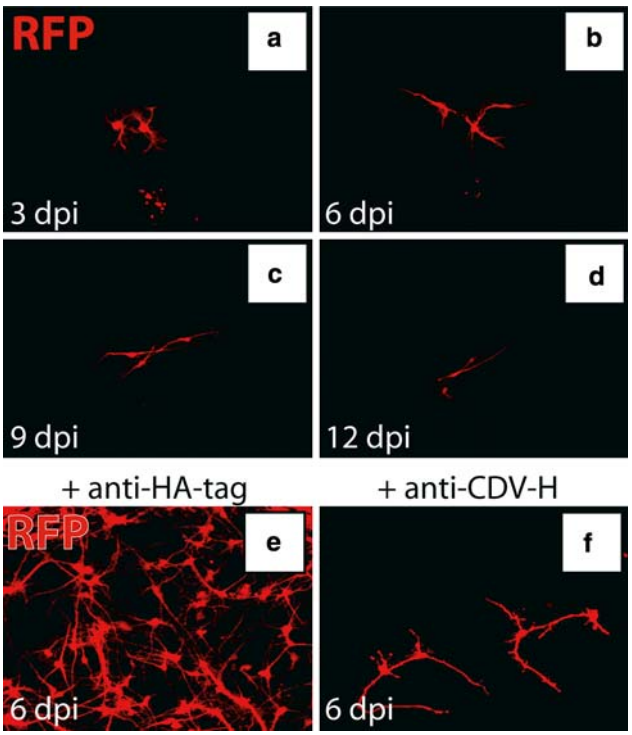

Fig. 8 Role of the receptor-binding H protein in viral spread. **a–d** Infection of DBCCs with a hemagglutinin (H) knockout, H *trans*-complemented recombinant A75/17 virus (rA75/17^{red}/H^{ko}/H^{comp}). The latter recombinant virus required initial *trans*-complementation with the wild-type hemagglutinin (Hwt) protein in Vero-SLAM cells stably expressing Hwt (Vero-SLAM-H cells). The four images taken at 3, 6, 9 and 12 dpi of the same infected focus illustrated no further spread from the initially infected cells. Infected cells were identified by capturing red fluorescence emission using a confocal laser microscope. **e**, **f** DBCCs infected with rA75/17^{red} and treated with an antibody against H (MAb 1347 [26]) exhibited markedly fewer infected cells as compared to cultures treated with a control antibody (MAb anti-HA). Infected cells were identified by capturing red fluorescence emission using a confocal laser microscope

DBCCs. Moreover, agar overlay of the cultures did not impair spread and electron microscopic examination illustrated ample presence of viral nucleocapsids in infected cells but extremely rare signs of budding or free viral particles. In addition, in an unanticipated manner, we demonstrated that consecutive spread between cells can happen within 5–6 h. It is interesting to note in this respect that Duprex and collaborators [7] demonstrated spread of MV in astrocytoma cell lines in a time frame of 4–5 h. These observations are hard to reconcile with the fact that it takes about 24 h for CDV to enter a cell, replicate, and release progeny particles to infect a new cell [12]. Taken together, these results strongly argue against extracellular transfer of viral particles as a way how persistent CDV is transmitted in astrocytes. Since at any time point all infected cells in a given area always seemed to be in contact with each other by way of their processes, direct intracellular transfer of infectious material between astrocytes is suggested.

Since spontaneous diffusion of RFP did not occur in non-infected, RFP-transfected (not shown) and, most importantly, in rA75/17^{red} H^{ko}/H^{comp}-infected canine brain cell cultures, pre-existing channels between normal astrocytes, if such exist at all, are presumably not employed for nucleocapsid transfer from one cell to another. Thus, we have to assume that the infection itself could induce such channels. This could happen using the morbillivirus membrane fusion machinery even though clear evidence for cell–cell fusion in the form of multinucleated syncytia is completely lacking in persistent CDV infection. Nevertheless, we demonstrated that persistent CDV expressed functional fusogenic complexes, which consist of the fusion (F) and attachment (H) glycoproteins at the plasma membrane of glial cells. These could only induce fusion following binding of the fusion complex to the viral receptor. We documented that such binding presumably took place since an H-knockout recombinant virus was totally defective in viral spread and treatment of infected cells with a monoclonal anti-H antibody dramatically reduced lateral cell-to-cell transmission. This is the first demonstration for CDV that persistent cell-to-cell spread in primary canine brain cells is very likely dependent on the receptor-binding H protein. Consequently, according to the current morbillivirus-induced fusion model, potential cell–cell fusion events would then require proper expression of a cellular receptor on target cells. Since we found that the universal *Morbillivirus* CD150/SLAM receptor was not expressed in glial cells, these results suggest the existence of a hitherto unknown CDV receptor on glial cells necessary to allow CDV intracellular spread. This stands in sharp contrast to persistent MV infection in rat neuronal cells, where non-cytolytic cell-to-cell viral transmission has been reported to depend on a target receptor for the initial cell entry but not for subsequent lateral spread [20]. On the other hand, we cannot definitely rule out that H is only required to bind a target receptor, in turn generating pores in an F-independent manner, or that H is necessary to help F to be transported to the cell surface in its potentially functional pre-fusion conformational state.

Taken together, our findings are suggestive for fusion activity induced by CDV between infected and target cells, which presumably result from the combination of the fusion complex and a viral receptor, to enable the virulent virus to spread in glial cells. However, since multinucleated cells were not observed in CDV-infected cells, fusion activity presumably must be limited to small areas of the cell membrane by some unknown molecular mechanisms. We thus hypothesize that only micro-fusion events are mediated by virulent CDV in infected glial cells. Such micro-fusion events have been postulated to occur in MV

infection in vitro [7, 9, 10] but have never been clearly demonstrated.

Confocal microscopical images of infected DBCCs in the present study were suggestive of continuity between infected cells by way of thin connecting cell processes, often containing nucleocapsids even in the thinnest astrocytic ramifications, as detected by electron microscopy and immunofluorescence analysis. Confirmation of continuity between infected cells with the electron microscope remains anecdotical because of low probability to cut two remote cells and a connecting cell process in the same plane of section. Other signs that could be indicative of membrane fusion activity included focal plasmalemmal densities or "spiking" of the viral glycoproteins, attachment of nucleocapsids to the cell membrane, and occasionally, blurring of the borders of opposing cell membranes. While unequivocal morphological demonstration of micro-fusion events based on static images remains elusive, their existence is, however, supported by our functional assays demonstrating that H was essential for CDV spread, in turn suggesting that the viral fusion complex was indeed of importance.

Our dynamic studies in living cultures clearly showed that viral transmission between infected and target cells occurred specifically at the tips of astrocytic processes. Therefore, CDV was rarely transmitted to immediately adjacent cells, even though DBCCs are completely confluent and often multilayered. Consequently, CDV spread obviously takes place along cell processes to remote cells bypassing numerous others, which remained uninfected, carrying the infection over large distances in the culture. While our observations explain why viral spread is indeed selective, as previously proposed in CDV [39] and in MV [8], how could the postulated micro-fusion events occur only in these very limited areas of the cell membrane? This might be related to specific cell membrane targeting of the viral glycoproteins as described in MV [23] or restricted distribution of the putative, yet unidentified, glial CDV receptor, perhaps similar to viral receptor clustering directing fusion in MV [35]. However, the extremely restricted targeting of the postulated viral fusion events in our study suggests that cellular factors must be involved. Selective spread of CDV in astrocytes is reminiscent of MV infections in selected neuronal networks using existing neuronal transport mechanisms or functional connections to spread [9, 21]. In ferrets, CDV can also use neuronal pathways to enter and spread in the brain [32]. However, specific to CDV in dogs and relevant to the demyelinating process is the infection of white matter astrocytes, the main target of CDV in vivo and in vitro [39]. Akin to neurons, astrocytes also establish communication networks in which gap junctions play a synapse-like role [14]. Since intercellular junctions have been shown to promote viral egress in other viral systems [13], it is quite possible that CDV uses perhaps the gap junctions, which are indeed concentrated at the tip of processes [31], to spread in the astrocytic syncytial network. How the viral fusion complex and its receptor interact with such astrocytic factors is subject of future work.

In conclusion, our findings indicated that persistent CDV infection can spread from cell-to-cell without using free viral particles. Moreover, our data suggested that spread probably requires interaction of the viral attachment protein at the surface of an infected cell with a yet unidentified glial cellular receptor on target cell. Although other mechanisms cannot be excluded, it seems reasonable to assume that this binding triggers the fusion protein to establish micro-pores between infected and target cells, allowing transfer of viral nucleocapsids.

Although it is thought that non-cytolytic cell-to-cell spread of viruses evolved to escape immune detection [34], CDV in the CNS is readily detected by the immune system [39]. Therefore, the neuropathology of distemper encephalitis is characterized by intense inflammation with clearance of the virus. It is important to note that this process is restricted to focal areas of the white matter. However, coexisting with and outside of these inflammatory plaques, clusters of infected astrocytes are found, thus showing continuing viral spread despite an effective intrathecal anti-viral immune response [39]. Our present findings may shed some light on this phenomenon which is clearly responsible for the chronic progression of the disease. They show that CDV can spread rapidly in the astrocytic network. By the time an effective immune response is mounted in an infected area, the virus is already carried away from the focus of anti-viral attack. Thus, viral persistence in CDV infection may be explained by a strategy of "outrunning" the immune response.

Acknowledgments We are grateful to P. Salmon, D. Garcin, C. Örvell and V. von Messling for having provided the pRRL lenti plasmid system, the RFP gene, monoclonal antibodies, and the Vero-SLAM cells, respectively. This work supported by the Ernst&Charlotte Frauchiger foundation.

References

1. Bollo E, Zurbriggen A, Vandevelde M, Fankhauser R (1986) Canine distemper virus clearance in chronic inflammatory demyelination. Acta Neuropathol (Berl) 72:69–73
2. Brettschneider J, Tumani H, Kiechle U, Muche R, Richards G, Lehmensiek V, Ludolph AC, Otto M (2009) IgG antibodies

against measles, rubella, and varicella zoster virus predict conversion to multiple sclerosis in clinically isolated syndrome. PLoS One 4:e7638
3. Brown HR, Goller N, Thormar H, Norrby E (1987) Fuzzy material surrounding measles virus nucleocapsids identified as matrix protein. Brief report. Arch Virol 94:163–168
4. Buchholz UJ, Finke S, Conzelmann KK (1999) Generation of bovine respiratory syncytial virus (BRSV) from cDNA: BRSV NS2 is not essential for virus replication in tissue culture, and the human RSV leader region acts as a functional BRSV genome promoter. J Virol 73:251–259
5. Calain P, Roux L (1993) The rule of six, a basic feature for efficient replication of Sendai virus defective interfering RNA. J Virol 67:4822–4830
6. Dayer AG, Jenny B, Sauvain MO, Potter G, Salmon P, Zgraggen E, Kanemitsu M, Gascon E, Sizonenko S, Trono D, Kiss JZ (2007) Expression of FGF-2 in neural progenitor cells enhances their potential for cellular brain repair in the rodent cortex. Brain 130:2962–2976
7. Duprex WP, McQuaid S, Hangartner L, Billeter MA, Rima BK (1999) Observation of measles virus cell-to-cell spread in astrocytoma cells by using a green fluorescent protein-expressing recombinant virus. J Virol 73:9568–9575
8. Duprex WP, McQuaid S, Roscic-Mrkic B, Cattaneo R, McCallister C, Rima BK (2000) In vitro and in vivo infection of neural cells by a recombinant measles virus expressing enhanced green fluorescent protein. J Virol 74:7972–7979
9. Ehrengruber MU, Ehler E, Billeter MA, Naim HY (2002) Measles virus spreads in rat hippocampal neurons by cell-to-cell contact and in a polarized fashion. J Virol 76:5720–5728
10. Firsching R, Buchholz CJ, Schneider U, Cattaneo R, ter Meulen V, Schneider-Schaulies J (1999) Measles virus spread by cell-cell contacts: uncoupling of contact-mediated receptor (CD46) downregulation from virus uptake. J Virol 73:5265–5273
11. Glaus T, Griot C, Richard A, Althaus U, Herschkowitz N, Vandevelde M (1990) Ultrastructural and biochemical findings in brain cell cultures infected with canine distemper virus. Acta Neuropathol 80:59–67
12. Higgins RJ, Krakowka S, Metzler AE, Koestner A (1982) Immunoperoxidase labeling of canine distemper virus replication cycle in Vero cells. Am J Vet Res 43:1820–1824
13. Johnson DC, Webb M, Wisner TW, Brunetti C (2001) Herpes simplex virus gE/gI sorts nascent virions to epithelial cell junctions, promoting virus spread. J Virol 75:821–833
14. Kielian T (2008) Glial connexins and gap junctions in CNS inflammation and disease. J Neurochem 106:1000–1016
15. Krone B, Oeffner F, Grange JM (2009) Is the risk of multiple sclerosis related to the 'biography' of the immune system? J Neurol 256:1052–1060
16. Lamb RA (1993) Paramyxovirus fusion: a hypothesis for changes. Virology 197:1–11
17. Lamb RA, Jardetzky TS (2007) Structural basis of viral invasion: lessons from paramyxovirus F. Curr Opin Struct Biol 17:427–436
18. Lamb RA, Kolakofsky D (2001) Paramyxoviridae: the viruses and their replication. In: Fileds BN, Knipe DM, Howley PM, Griffin DE (eds) Fields virology, 4th edn. Lippincott-Raven Publishers, Philadelphia, PA, pp 1305–1340
19. Lassmann H, Bruck W, Lucchinetti CF (2007) The immunopathology of multiple sclerosis: an overview. Brain Pathol 17:210–218
20. Lawrence DM, Patterson CE, Gales TL, D'Orazio JL, Vaughn MM, Rall GF (2000) Measles virus spread between neurons requires cell contact but not CD46 expression, syncytium formation, or extracellular virus production. J Virol 74:1908–1918
21. Makhortova NR, Askovich P, Patterson CE, Gechman LA, Gerard NP, Rall GF (2007) Neurokinin-1 enables measles virus trans-synaptic spread in neurons. Virology 362:235–244
22. Marq JB, Brini A, Kolakofsky D, Garcin D (2007) Targeting of the Sendai virus C protein to the plasma membrane via a peptide-only membrane anchor. J Virol 81:3187–3197
23. Moll M, Pfeuffer J, Klenk HD, Niewiesk S, Maisner A (2004) Polarized glycoprotein targeting affects the spread of measles virus in vitro and in vivo. J Gen Virol 85:1019–1027
24. Muller CF, Fatzer RS, Beck K, Vandevelde M, Zurbriggen A (1995) Studies on canine distemper virus persistence in the central nervous system. Acta Neuropathol (Berl) 89:438–445
25. Orlando EA, Imbschweiler I, Gerhauser I, Baumgartner W, Wewetzer K (2008) In vitro characterization and preferential infection by canine distemper virus of glial precursors with Schwann cell characteristics from adult canine brain. Neuropathol Appl Neurobiol 34:621–637
26. Orvell C, Sheshberadaran H, Norrby E (1985) Preparation and characterization of monoclonal antibodies directed against four structural components of canine distemper virus. J Gen Virol 66(Pt 3):443–456
27. Plattet P, Rivals JP, Zuber B, Brunner JM, Zurbriggen A, Wittek R (2005) The fusion protein of wild-type canine distemper virus is a major determinant of persistent infection. Virology 337:312–326
28. Plattet P, Zweifel C, Wiederkehr C, Belloy L, Cherpillod P, Zurbriggen A, Wittek R (2004) Recovery of a persistent Canine distemper virus expressing the enhanced green fluorescent protein from cloned cDNA. Virus Res 101:147–153
29. Rima BK, Duprex WP (2006) Morbilliviruses and human disease. J Pathol 208:199–214
30. Rivals JP, Plattet P, Currat-Zweifel C, Zurbriggen A, Wittek R (2007) Adaptation of canine distemper virus to canine footpad keratinocytes modifies polymerase activity and fusogenicity through amino acid substitutions in the P/V/C and H proteins. Virology 359:6–18
31. Rouach N, Koulakoff A, Abudara V, Willecke K, Giaume C (2008) Astroglial metabolic networks sustain hippocampal synaptic transmission. Science 322:1551–1555
32. Rudd PA, Cattaneo R, von Messling V (2006) Canine distemper virus uses both the anterograde and the hematogenous pathway for neuroinvasion. J Virol 80:9361–9370
33. Russell CJ, Jardetzky TS, Lamb RA (2001) Membrane fusion machines of paramyxoviruses: capture of intermediates of fusion. EMBO J 20:4024–4034
34. Sattentau Q (2008) Avoiding the void: cell-to-cell spread of human viruses. Nat Rev Microbiol 6:815–826
35. Singethan K, Muller N, Schubert S, Luttge D, Krementsov DN, Khurana SR, Krohne G, Schneider-Schaulies S, Thali M, Schneider-Schaulies J (2008) CD9 clustering and formation of microvilli zippers between contacting cells regulates virus-induced cell fusion. Traffic 9:924–935
36. Sips GJ, Chesik D, Glazenburg L, Wilschut J, De Keyser J, Wilczak N (2007) Involvement of morbilliviruses in the pathogenesis of demyelinating disease. Rev Med Virol 17:223–244
37. Tatsuo H, Ono N, Tanaka K, Yanagi Y (2000) SLAM (CDw150) is a cellular receptor for measles virus. Nature 406:893–897
38. Tatsuo H, Ono N, Yanagi Y (2001) Morbilliviruses use signaling lymphocyte activation molecules (CD150) as cellular receptors. J Virol 75:5842–5850
39. Vandevelde M, Zurbriggen A (2005) Demyelination in canine distemper virus infection: a review. Acta Neuropathol (Berl) 109:56–68
40. von Messling V, Milosevic D, Cattaneo R (2004) Tropism illuminated: lymphocyte-based pathways blazed by lethal morbillivirus through the host immune system. Proc Natl Acad Sci USA 101:14216–14221

41. von Messling V, Svitek N, Cattaneo R (2006) Receptor (SLAM [CD150]) recognition and the V protein sustain swift lymphocyte-based invasion of mucosal tissue and lymphatic organs by a morbillivirus. J Virol 80:6084–6092
42. Wenzlow N, Plattet P, Wittek R, Zurbriggen A, Grone A (2007) Immunohistochemical demonstration of the putative canine distemper virus receptor CD150 in dogs with and without distemper. Vet Pathol 44:943–948
43. Zurbriggen A, Graber HU, Vandevelde M (1995) Selective spread and reduced virus release leads to canine distemper virus persistence in the nervous system. Vet Microbiol 44:281–288
44. Zurbriggen A, Graber HU, Wagner A, Vandevelde M (1995) Canine distemper virus persistence in the nervous system is associated with noncytolytic selective virus spread. J Virol 69:1678–1686